

# Structural Analysis of Dispersion Strengthened Material on Aluminium Base

Mária Orolínová, Juraj Ďurišin, Katarína Ďurišinová, Michal Besterci, Karel SaksI

*Institute of Materials Research of Slovak Academy of Sciences,  
Watsonova 47, 043 53 Košice, Slovak Republic*

(Received January 15, final form January 23, 2009)

## ABSTRACT

Dispersion strengthened materials are characterized by high strength properties and good temperature stability of structure until to temperatures of 0.9 melting temperature of aluminium. Dispersion strengthened Al -  $\text{Al}_4\text{C}_3$  materials are prepared by powder metallurgy way and the raw powder mixtures are generally consolidated by hot extrusion obtaining a fully dense material. This work is focused on a study of the microstructure in Al -  $\text{Al}_4\text{C}_3$  materials containing 4 and 12 vol. %  $\text{Al}_4\text{C}_3$ . The microstructure was analyzed by transmission electron microscopy and X-ray diffraction methods. The several microstructural features: morphology, size and distribution of particles of dispersoid, grain size and crystallite size of aluminium matrix, micro strain and dislocations density in materials were determined. The aim is an analysis of the effect of  $\text{Al}_4\text{C}_3$  amount on the microstructure formation during hot extrusion and analysis of the microstructure evolution at temperature loading and after cooling to ambient temperature.

After hot extrusion the Al - 12 vol. %  $\text{Al}_4\text{C}_3$  alloy is characterized by finer grains, higher micro strain and dislocations density and by a very low intensity of aluminium matrix deformation texture in comparison to Al - 4 vol. %  $\text{Al}_4\text{C}_3$  material. In the hot extruded system with 4 vol. %  $\text{Al}_4\text{C}_3$  a strong deformation texture was observed. Therefore the amount of dispersoid strongly affects the formation of microstructures. The higher volume of  $\text{Al}_4\text{C}_3$  particles provides effective hindrance of the dislocations motion in Al matrix by the attractive interaction between dislocations and particles during

extrusion. Both amounta of  $\text{Al}_4\text{C}_3$  dispersoid insure the thermal stability of microstructure of analyzed materials to 773 K.

## 1. INTRODUCTION

Aluminium alloys possess an attractive combination of properties: low specific gravity, high strength, excellent corrosion resistance and good machinability. A major drawback of aluminium-base alloys is their low heat resistance. Using aluminium alloys at temperatures above 473 K is practically impossible. In this connection, great interest is attached to the development of dispersion strengthened aluminium materials capable of maintaining their strength properties on heating to temperatures of 0.9 melting temperature of aluminium /1/. Dispersion strengthened aluminium materials offer significant performance advantages over pure aluminium and aluminium alloys. The desirable properties of these materials give them many potential applications in areas such as in the automotive and aerospace industries.

In the dispersion strengthened composites, nanoparticles – dispersoid are added to the matrix material. The addition of a small amount of very hard and thermally stable, incoherent particles of a secondary phase with a suitable distribution in 3D matrix acts toward matrix strengthening and retains the strengthening action at elevated temperatures /2/. Various processes have been used to develop these composites, such as mechanical alloying/powder

metallurgy, “in situ” formation of dispersoids via a chemical reaction within the matrix phase /3/. To obtain a homogeneous distribution of nano-sized dispersoids in such a ductile matrix a reaction milling is susceptible. Reaction milling is a variant of mechanical alloying. Suitable dispersoids can be formed by a solid state reaction by introducing components that react with the matrix particular during milling and mainly during the subsequent heat treatment. In the case of Al alloys the introduction of graphite is most successful /4/. The carbon introduced by milling reacts with Al to form fine and well distributed  $Al_4C_3$  particles. Generally the raw powder mixtures are consolidated by hot extrusion or by hot isostatic pressing obtaining a fully dense material. The purpose of this work is to investigate the influence of the different amount of  $Al_4C_3$  dispersoid on the extruded Al matrix microstructure and on the temperature stability of microstructure by means the transmission electron microscopy (TEM) and X-ray diffraction (XRD) analyses. These methods are not alternatives for characterizing the structure, but they provide different aspects of the microstructure.

## 2. EXPERIMENTAL PROCEDURE

The experimental materials were prepared by the method of mechanical alloying. Al powder of powder particle size below of 50  $\mu m$  was dry milled in an attritor for 90 min with the addition of graphite KS 2.5 thus creating 4 and 12 vol. % of  $Al_4C_3$ . Then the specimens were cold pressed using a load of 600 MPa. The specimens had cylindrical shape. Subsequent heat treatment at 823 K for 3 h induced chemical reaction  $4Al + 3C \rightarrow Al_4C_3$ . Next the cylinders were hot extruded at 873 K with 94 % reduction of the cross section. Due to a high affinity of Al to  $O_2$  the system also contains a small amount of  $Al_2O_3$  particles (ca 1 vol. %). They are formed during the reaction milling in attritors. The residual porosity in this material was considerably up to 1 %. The both extruded specimens in the longitudinal and cross direction with respect to the direction of extrusion were analyzed by the TEM and XRD analyses.

TEM analyses were realized for both materials after the extrusion and after their annealing at temperature

773 K during 1 h. Geometrical and morphological parameters of secondary phases were investigated. The mean diameter of secondary particles was recovered by the direct measuring of statistical file ca 200 particles on thin TEM foils. The mean free path between particles was estimated by the equation for mono dispersion set of spherical particles:

$$\Lambda = 2d(1 - f)/3f, \quad (1)$$

where  $\Lambda$  is the particles space,  $d$  is the mean particles diameter and  $f$  is the volume fraction of particles. The grain size of Al matrix was directly measured on the TEM foils too.

The qualitative phase analyses, micro-strain, crystallite size and corresponding dislocations density were analyzed using the X-ray diffraction methods. The X-ray diffraction patterns were obtained by Philips X'Pert Pro powder diffractometer equipped with Ni-filtered  $CuK\alpha$  radiation using the positional sensitive detector X'Celerator and High temperature Camera up to 1873 K (HTK 16). The measurements were realized at the ambient temperature, in-situ during thermal exposition at 773 K during 1 hour and after cooling to the ambient temperature. The full widths at half maximum (FWHM), intensities of measured diffraction peak and qualitative phase analyses were determined with using the High Score program and PDF 2 (Powder Diffraction File). The micro-strains, crystallite sizes and dislocations densities were determined by the diffraction line broadening analysis using Hall and Williamson-Smallman equations /5, 6/. Texture coefficients were calculated from the X-ray diffraction data using a following equation. /7/.

$$TC_{hkl} = \frac{I_{hkl}/I_{0hkl}}{1/n \sum_{i=1}^n (I_{hkl}/I_{0hkl})}, \quad (2)$$

where  $TC_{hkl}$  is the texture coefficient for the reflection (hkl),  $I_{hkl}$  is the relative diffraction intensity of (hkl) diffraction peak from the experimental data,  $I_{0hkl}$  is the standard peak intensity for the reflection (hkl) according to reference file.

### 3. RESULTS AND DISCUSSION

#### 3.1 TEM analysis

TEM is probably one of the most direct methods to determine the character of the microstructure. Typical examples of the TEM micrographs of as-extruded Al – 4 vol. %  $\text{Al}_4\text{C}_3$  composite in longitudinal section to the extrusion direction are given in Fig. 1. Figure 2 documents the TEM microstructure of Al – 12 vol. %  $\text{Al}_4\text{C}_3$  in the longitudinal section. The secondary phases are distributed in both extruded experimental materials in cross direction homogeneously in the aluminium matrix. In longitudinal direction the  $\text{Al}_4\text{C}_3$  particles are placed in parallel rows as a consequence of extrusion. Morphologically,  $\text{Al}_4\text{C}_3$  particles are elongated but they have only a low aspect ratio, so that they can be approximated as spherical. The  $\text{Al}_4\text{C}_3$  particles in this materials can be divided into two distinctive groups: A – very fine particles with mean diameter size approximately 30 nm and B – large particles, that are mostly formatted by aggregates of particles (with diameter size to 500 nm). The large particles are not effective in term of dispersion strengthening. Their amount is around 5 % from the total amount of the  $\text{Al}_4\text{C}_3$  particles in the Al – 4 vol. %  $\text{Al}_4\text{C}_3$  and 10 % in the Al – 12 vol. %  $\text{Al}_4\text{C}_3$  materials. Consequently the effective volume of  $\text{Al}_4\text{C}_3$  particles introduces 3, 96 % in the material with 4 vol. %  $\text{Al}_4\text{C}_3$  and in the material with 12 vol. %  $\text{Al}_4\text{C}_3$  is 10, 8 %. These small particles generally bond well with the matrix and act to help the matrix resist deformation and this makes the material stronger. The matrix is carrying most of the load and the deformation accomplish by slip and movement of dislocation [9]. The mean free path between particles appertains to the fundamental structural parameters incident the distribution of dispersoid in the dispersion strengthened systems. Because the mean particles diameter of the effective secondary strengthened phase is equal in both materials, the mean free path depends only on the volume amount of the particles. The mean free path (according to equation 1) of the effective dispersion strengthening  $\text{Al}_4\text{C}_3$  particles is 485 nm in the material with 4 vol. %  $\text{Al}_4\text{C}_3$  and 165 nm in the material with 12 vol. %  $\text{Al}_4\text{C}_3$ .

The microstructure of the system with 4 vol. %  $\text{Al}_4\text{C}_3$  in longitudinal direction consists of grains fine elongated parallel to the extrusion direction (Fig. 1).

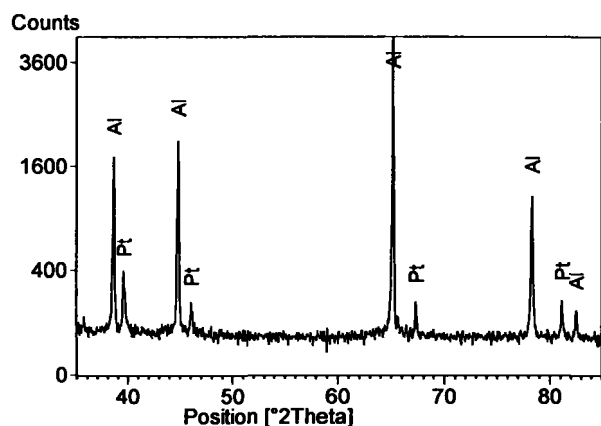
Then relative low amount of effective strengthened particles and limited value of the particles spacing cannot suppress the sliding of the grain boundaries during extrusion. In perpendicular section to the pressing direction the grains seem approximately equiaxed. The microstructure of the material with 12 vol. %  $\text{Al}_4\text{C}_3$  consists of approximately equiaxial grains that are similar in both sections (Fig. 2). Thus this material is not characterized by the preferential grain orientation. Larger amount of the effective particles of the secondary phase and a lower interparticles spacing in comparison with the material Al – 4 vol. %  $\text{Al}_4\text{C}_3$  impede the sliding of the grain boundaries in the process of the extrusion. The dislocations are stabilized and pinned down at the particles. Because the presence of the fine  $\text{Al}_2\text{O}_3$  particles in the microstructure of both materials was confirmed [8], dispersion strengthening of the Al matrix is involved with these particles too.

Figures 3 and 4 show TEM micrographs of a longitudinal direction of both as-extruded materials after annealing at 773 K for the duration of 1 h. The size, distribution and morphology of the secondary phases, as well as the parameters of grains are unchanged in both cases after annealing at 773 K.  $\text{Al}_4\text{C}_3$  particles are stable and do not tend to coarsen at elevated temperatures.

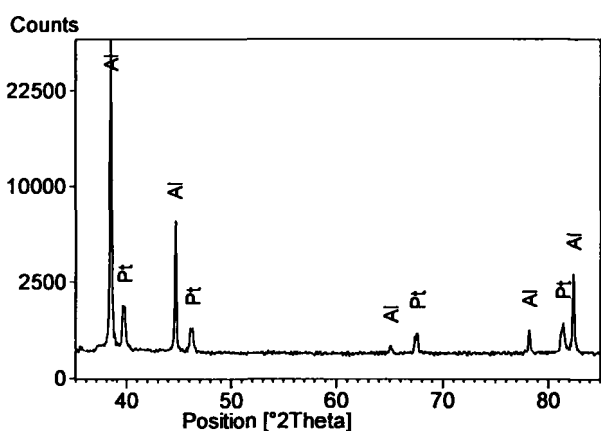
#### 3.2 X – ray analysis

##### 3.2.1 Qualitative phase analysis

Figure 5a documents the XRD lines courses in the longitudinal direction as-extruded Al – 4 vol. %  $\text{Al}_4\text{C}_3$  material at the ambient temperature and Fig. 5b shows the XRD lines courses in the cross direction. The qualitative phase analyses of the diffraction spectra measured at the ambient temperature confirmed the lines of aluminium and platinum. The presence of the platinum reflections is in consequence of platinum heating body on which is the sample located (by reason of consistent measurements at higher temperatures). The presence of  $\text{Al}_4\text{C}_3$  phase was not recorded in this experimental material. This fact can be caused by the low amount of  $\text{Al}_4\text{C}_3$  phase (non-detected by X-ray analysis) and homogeneously distribution of very fine  $\text{Al}_4\text{C}_3$  particles in the Al matrix. Indexed phases in Figs. 5a and 5b confirmed according to JCPDS (International Centre for Diffraction Data) reference file: aluminium 04-487, platinum 04-0802.



5(a)



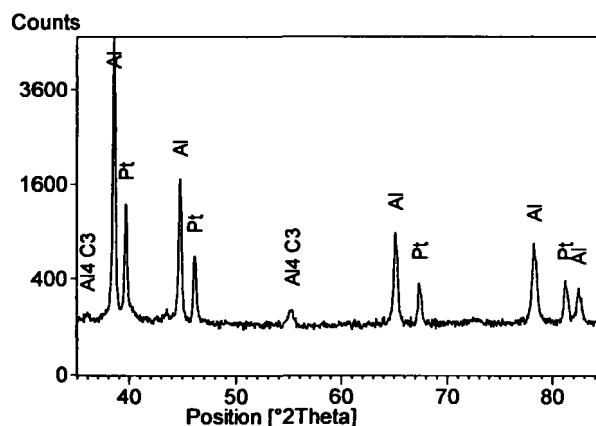
5(b)

**Fig. 5a,b:** XRD spectrum of the Al – 4 vol. %  $\text{Al}_4\text{C}_3$  material scanned at the ambient temperature and the phase analysis: a) longitudinal direction, b) cross direction

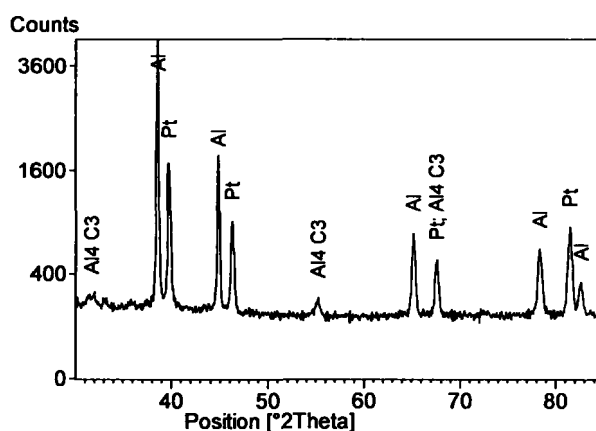
Figure 6a shows the XRD lines courses in the longitudinal direction as-extruded Al – 12 vol. %  $\text{Al}_4\text{C}_3$  material at the ambient temperature and Fig. 6b shows the XRD lines courses in the cross direction. In this material the qualitative phase analysis of diffraction spectra confirmed besides the lines of aluminium, platinum moreover aluminium carbide. Indexed phases in Figs. 5 and 6 confirmed according to JCPDS reference file: aluminium 04-487, platinum 04-0802 and aluminium carbide 01-0953.

### 3.2.2 X-ray profile analysis

X-ray line profile analysis is a powerful tool for determining the micro-strains, grain or crystallite size



6(a)



6(b)

**Fig. 6a,b:** XRD spectrum of the Al – 12 vol. %  $\text{Al}_4\text{C}_3$  material scanned at the ambient temperature and the phase analysis: a) longitudinal direction, b) cross direction

and dislocations densities. These parameters are fundamental features related to the microstructure [10]. In comparison with TEM the X-ray method provides average values with better statistics of the different parameters of the microstructure. The crystallite size  $D$  and the corresponding micro-strains  $\epsilon$  were measured for using diffraction line broadening methods because both these parameters are related to the size broadening of diffraction lines. The crystallite size and the micro strain effects on the diffraction peak broadening can be evaluated separately on the basis of their different  $hkl$  dependences. Both these parameters were determined by means of Hall and Williamson-Smallman equations [5, 11]. The measurements were realized on both

experimental as-extruded materials at the ambient temperature, in situ at 773 K and after cooling to the ambient temperature. In Fig. 7a the XRD lines courses from Al – 4 vol. %  $\text{Al}_4\text{C}_3$  material at all temperatures are compared in the longitudinal direction and in Fig. 7b in the cross direction. Figs. 8a and 8b documents these diffraction lines for Al – 12 vol. %  $\text{Al}_4\text{C}_3$  material. Tables 1 and 2 show the determined values of the crystallites sizes, micro-strains and dislocations densities for both materials at different temperatures.

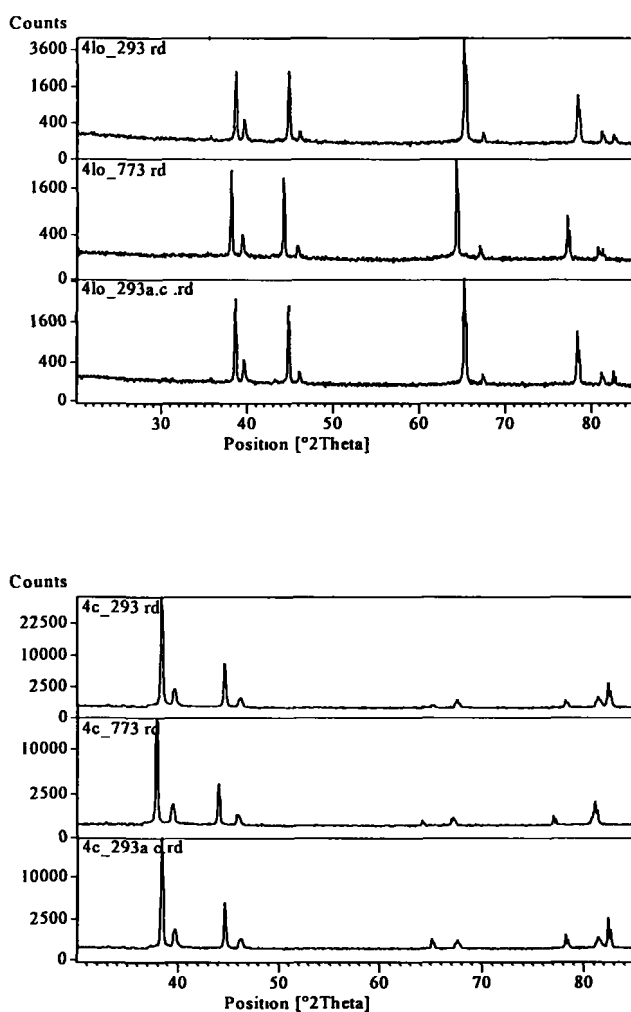


**Fig. 7:** XRD spectrum of the Al – 4 vol. %  $\text{Al}_4\text{C}_3$  material scanned at the ambient temperature, at 773 K and after cooling to the ambient temperature; a) longitudinal direction, b) cross direction

The crystallite size of the Al matrix in the material with 4 vol. %  $\text{Al}_4\text{C}_3$  at the ambient temperature is in range 72-218 nm and in the material with 12 vol. %  $\text{Al}_4\text{C}_3$  is in interval 61-106 nm, Tables 1 and 2. It has to be mentioned that the crystallite size determined by the X-ray profile analysis relates to a size of coherently scattering areas. Consequently, the grain size determined by X-ray diffraction analysis is smaller than the grain size determined from the TEM images. This difference can be explained by the sensitivity of the XRD method to small misorientation and dislocation dipoles [12]. Material Al – 12 vol. %  $\text{Al}_4\text{C}_3$  is characterized by smaller crystallite size measured at the ambient temperature in comparison with material Al – 4 vol. %  $\text{Al}_4\text{C}_3$ , Tables 1 and 2. It is clear that the crystallite size measured by the X-ray diffraction is much smaller than the grain size observed in the TEM images as shown in Figs. 1-4. In the material Al – 4 vol. %  $\text{Al}_4\text{C}_3$ , expressive difference in the crystallite size is observed in the case of (111) and (222) slip planes whereas in the material with 12 vol. %  $\text{Al}_4\text{C}_3$  this difference is smaller. This can be explained thereby the higher amount of fine  $\text{Al}_4\text{C}_3$  particles being effective in storing dislocations in the Al matrix and in suppressing their annihilation and blocking the cross-slip and thermally activated climbing during the process of hot extrusion. By in situ measuring at 773 K the mean crystallite sizes grow in both materials in comparison to the initial state. After cooling to the ambient temperature the mean matrix crystallite size grows only minor in the material with 4 vol. %  $\text{Al}_4\text{C}_3$  in comparison to the initial state. Mean crystallite size nevertheless decreases in compare to the initial state in material with 12 vol. %  $\text{Al}_4\text{C}_3$ .

The micro-strain achieves the mean value about  $1 \cdot 10^{-3}$  in the as-extruded material Al- 4 vol. %  $\text{Al}_4\text{C}_3$  and approximately  $1.3 \cdot 10^{-3}$  in the material Al - 12 vol. %  $\text{Al}_4\text{C}_3$ . Micro- and nano-structured materials often exhibit high level of micro-strain [13]. Micro-strain determined from the XRD peak broadening represents the concentration of lattice defects (mainly dislocations) in the sample. The dislocation density comes up to place value  $10^{14} \text{ m}^{-2}$  in both experimental materials in the state after extrusion. The high density of the dislocations suggests that during mechanical alloying, at the milling

**Table 1**

The microstrain, crystallite size and dislocations density of the as-extruded Al – 4 vol. %  $\text{Al}_4\text{C}_3$  material measured at 293 K, 773 K and after cooling to 293 K (a.c.)

Al - 4 vol. % $\text{Al}_4\text{C}_3$									
Temperature [K]									
	293	773	a.c.	293	773	a.c.	293	773	a.c.
hkl	Microstrain $\varepsilon \cdot 10^{-3}$			Crystallite size D [nm]			Dislocations density $\rho$ [ $\text{m}^{-2}$ ]		
111	0.8	0.5	0.7	218.3	389.6	248.6	$6.3 \cdot 10^{13}$	$2.0 \cdot 10^{13}$	$4.9 \cdot 10^{13}$
200	1.1	0.6	1.0	122.6	246.1	141.5	$2.0 \cdot 10^{14}$	$4.9 \cdot 10^{13}$	$1.5 \cdot 10^{14}$
220	1.1	0.5	1.2	81.2	190.3	77.6	$4.6 \cdot 10^{14}$	$8.3 \cdot 10^{13}$	$5.0 \cdot 10^{14}$
311	1.0	0.5	1.0	72.3	160.5	75.9	$5.7 \cdot 10^{14}$	$1.2 \cdot 10^{14}$	$5.2 \cdot 10^{14}$
222	0.6	0.4	1.2	135.1	249.8	150.0	$1.6 \cdot 10^{14}$	$4.8 \cdot 10^{13}$	$1.3 \cdot 10^{14}$
mean size	0.9	0.5	1.0	125.9	247.3	138.7	$2.6 \cdot 10^{14}$	$6.4 \cdot 10^{13}$	$2.7 \cdot 10^{14}$

**Table 2**

The microstrain, crystallite size and dislocations density of the as-extruded Al – 12 vol. %  $\text{Al}_4\text{C}_3$  material measured at 298 K, 773 K and after cooling to 298 K (a.c.)

Al - 12 vol. % $\text{Al}_4\text{C}_3$									
Temperature [K]									
	293	773	a.c.	293	773	a.c.	293	773	a.c.
hkl	Microstrain $\varepsilon \cdot 10^{-3}$			Crystallite size D [nm]			Dislocations density $\rho$ [ $\text{m}^{-2}$ ]		
111	1.4	0.9	1.4	106.7	197.8	108.7	$2.6 \cdot 10^{14}$	$7.7 \cdot 10^{13}$	$2.5 \cdot 10^{14}$
200	1.4	0.8	1.7	94.3	190.1	75.9	$3.4 \cdot 10^{14}$	$8.3 \cdot 10^{13}$	$5.0 \cdot 10^{14}$
220	1.3	0.5	1.3	65.2	191.7	64.4	$7.1 \cdot 10^{14}$	$8.2 \cdot 10^{13}$	$7.2 \cdot 10^{14}$
311	1.1	0.5	1.2	64.9	166.6	59.7	$7.1 \cdot 10^{14}$	$1.1 \cdot 10^{14}$	$8.4 \cdot 10^{14}$
222	1.1	0.5	1.2	61.6	183.8	57.4	$7.9 \cdot 10^{14}$	$3.0 \cdot 10^{13}$	$9.1 \cdot 10^{14}$
mean size	1.3	0.7	1.4	78.6	186.0	73.2	$5.6 \cdot 10^{14}$	$7.6 \cdot 10^{13}$	$6.4 \cdot 10^{14}$

of powders, the work hardening state is developed in the present alloys. In as-extruded material with 4 vol. % dispersoid the smallest micro-strain and dislocations density is observed in the case of (111) and (222) slip planes. On the contrary, no micro-strain and dislocations density decrease was observed on slip planes in material with 12 vol. % dispersoid. These results are in agreement with the observed decreasing subgrain sizes. The examined alloys were finally extruded at 773 K. This may imply that their microstructure including density and distribution of dislocations should be stable for heating up to this temperature. However, the dislocation density and micro strain decrease notably during the high-

temperature straining, Tables 1 and 2, probably due to the dynamic recovery. After cooling to the ambient temperature all measured parameters return in both materials on previous values, Tables 1 and 2. This can be explained by the influence of the thermal stresses arising at the interface boundaries during the cooling due to the difference between the thermal expansion coefficient of the matrix ( $\alpha = 23.5\text{--}26.5 \times 10^{-6} \text{ K}^{-1}$ ) and the particles ( $\alpha = 5 \times 10^{-6} \text{ K}^{-1}$ ). If these thermal stresses are high enough, dislocations are produced in dispersion strengthen materials near particles. The thermal stresses are dependant on the dispersoid size, particles space too.

### 3.2.3 Texture

The XRD spectra of the samples with 4 vol. %  $\text{Al}_4\text{C}_3$

after extrusion, measured at the ambient temperature in the both directions, Figs. 7a and 7b, exhibit reflexes due to (111), (200), (220), (311) and (222) planes of the aluminium. The degree of orientation of the different planes is not similar. The measured intensities of the individual aluminium diffraction peaks in these figures are not conformable with the relative intensities of the aluminium standard but they are markedly different, which suggests that after plastic forming - extrusion the material is characterized by the preferred orientation, or texture. The calculated values of the TCs are in Table 3. For a preferentially oriented sample, the texture coefficient  $TC_{(hkl)}$  should be greater than one. In the cross direction of this material  $TC_{111}$  and  $TC_{222}$  are the and in the longitudinal direction  $TC_{220}$  is the largest. The planes (220) and (222) are the secondary reflection planes of (110) and (111), respectively. Consequently, in the cross direction Al (111) and in the longitudinal direction Al (110) are dominated crystal orientations. The high values of the texture coefficients for (111) plane in the cross direction and for (110) plane in the longitudinal direction indicate the presence of marked deformation texture in the material. The presence of 4 vol. %  $Al_4C_3$  particles with mean size 30 nm and mean

free path between particles 485 nm in the Al matrix is not able to prevent aluminium crystalline lattices rotation during the extrusion. This amount of the secondary phase so cannot prevent the texture formation under the used conditions for the extrusion in our experimental alloy.

Figures 7a and 7b presents the comparison of the XRD spectrum in the cross and longitudinal direction for the extruded Al – 4 vol. %  $Al_4C_3$  material, obtained at 773 K and after cooling to the ambient temperature too. From this it is evident, that the intensities proportions of the individual aluminium reflections in the extruded materials are approximately identical at all measured temperatures, what implies that during and after thermal loading the texture is unchanged. The calculated values of the TCs at the single temperatures are documented in Table 3. The Al (111) orientation in the cross direction and Al (110) orientation in the longitudinal direction remain unchanged at the thermal loading at 773 K and after cooling to the ambient temperature in comparison to the sample after extrusion. In the alloy with 4 vol. %  $Al_4C_3$  strong extrusion texture was developed at used conditions of the extrusion. The texture after extrusion is stable to 773 K.

**Table 3**

The texture coefficients of the as-extruded Al – 4 vol. %  $Al_4C_3$  material measured at 293 K, 773 K and after cooling to 293 K (a.c.)

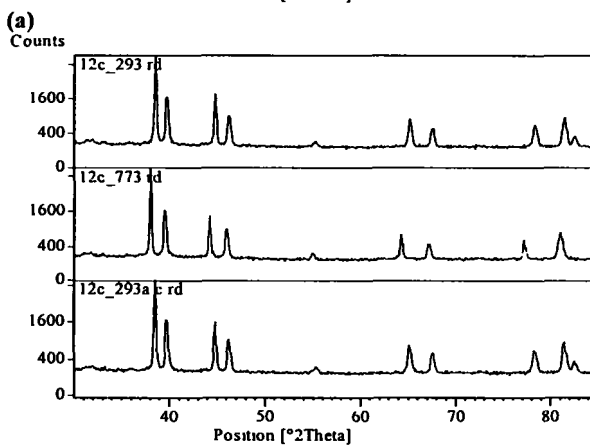
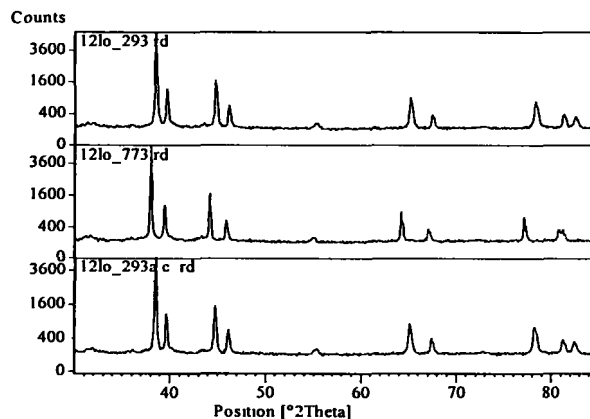
Al – 4 vol. % $Al_4C_3$							
Temperature [K]							
hkl	293	773	293 a. c.	hkl	293	773	293 a. c.
TC							
Cross section				Longitudinal section			
(111)	1.79	1.85	1.54	(111)	0.27	0.43	0.38
(200)	0.77	0.80	0.69	(200)	0.68	0.92	0.72
(220)	0.04	0.07	0.14	(220)	3.09	2.71	2.79
(311)	0.11	0.15	0.23	(311)	0.73	0.64	0.79
(222)	2.3	2.11	2.4	(222)	0.23	0.30	0.31

Figure 8a documents the diffraction lines course in the longitudinal direction for the extruded experimental material Al - 12 vol. %  $Al_4C_3$  at the ambient temperature and Fig. 8b presents the diffraction lines course in the cross direction. Contrary intensities of

aluminium diffraction lines of the Al - 4 vol. %  $Al_4C_3$ , Figs. 8a and 8b, approach the intensities of Al standard and the degree of orientation of the different planes in both directions is similar. Calculated values of the texture coefficients for this material in both directions

are shown in Table 4. The  $TC_{111}$  values in both directions are the highest, but all texture coefficients in this material approximate to 1. It is possible to say that the used conditions for the extrusion process have induced the deformation of the aluminium texture very low in the experimental alloy. The presence of 12 vol. % of  $Al_4C_3$  particles would prevent crystalline lattices rotation during mechanical work, such as extrusion, and consequently the texture development. Therefore the larger amount of  $Al_4C_3$  particles with mean size 30 nm and mean free path between particles 165 nm in the Al matrix produces a barrier that it hinders the deformation texture formation.

The X-ray diffraction lines of the sample Al - 12 vol. %  $Al_4C_3$  in the cross and longitudinal extrusion direction measured at the ambient temperature, at 773 K and after cooling to the ambient temperature shows Figs. 8a and 8b. The intensities proportions of the individual aluminium reflections in the extruded materials are approximately identical at all measured temperatures. Calculated values of the texture coefficients for this material in both directions are shown in Table 4. The presence of the 12 vol. %  $Al_4C_3$  particles in the Al matrix may hinder and even block grain boundary movement and suppress the deformation texture formation during the extrusion as well as the recrystallization texture formation during the temperature loading at 773 K of extruded material.



(b)  
Fig. 8: XRD spectrum of the Al – 12 vol. %  $Al_4C_3$  material scanned at the ambient temperature, at 773 K and after cooling to the ambient temperature; a) longitudinal direction, b) cross direction

Table 4

The texture coefficients of the as-extruded Al – 12 vol. %  $Al_4C_3$  material measured at 293 K, 773 K and after cooling to 293 K (a.c.)

Al – 12 vol. % $Al_4C_3$							
Temperature [K]							
hkl	293	773	293 a. c.	hkl	293	773	293 a. c.
TC							
Cross section				Longitudinal section			
(111)	1.39	1.32	1.35	(111)	1.32	1.47	1.40
(200)	0.89	0.84	0.89	(200)	0.92	0.88	0.96
(220)	1.13	1.13	1.09	(220)	1.07	1.07	1.03
(311)	0.81	0.80	0.68	(311)	0.76	0.74	0.82
(222)	0.79	0.90	0.96	(222)	0.93	0.84	0.80



#### 4. CONCLUSIONS

1. TEM analyses of the dispersion strengthened material Al – 4 vol. %  $\text{Al}_4\text{C}_3$  shows that its microstructure consists of grains fine elongated parallel to the extrusion direction. X-ray diffraction analyses establish that the crystallite size of the Al matrix in this material after extrusion ranges from 72 to 218 nm. The micro-strain achieves values ranging from 0.6 to  $1.1 \cdot 10^{-3}$  and the dislocation density has values from  $6.3 \cdot 10^{13}$  to  $5.7 \cdot 10^{14} \text{ m}^{-2}$ . These several microstructural features correlated with one another and the expressive differences in the values of all particular characteristics are observed in the case of (111) slip planes. The strong texturing is observed for (111) planes in the cross direction and for (110) in the longitudinal direction in this material. The amount of 4 vol. %  $\text{Al}_4\text{C}_3$  with the mean particle size 30 nm and mean free path between particles 485 nm stabilizes insufficiently the dislocation motion in Al matrix during hot extrusion process.

TEM analyses of the dispersion strengthen material Al – 12 vol. %  $\text{Al}_4\text{C}_3$  indicate that its microstructure creates fine equiaxed grains in both extrusion directions. The mean crystallite size is smaller in comparison to the material with 4 vol. %  $\text{Al}_4\text{C}_3$  ( $D=78 \text{ nm}$ ), the mean micro-strain and dislocation density are higher ( $\epsilon \cdot 10^3=1.3$ ,  $\rho \cdot 10^{14}=5.6 \text{ m}^{-2}$ ). The observed decrease in the grain size and increase in the dislocation density with increasing dispersoid content emphasize the positive role of  $\text{Al}_4\text{C}_3$  particles for the formation of an nanocrystalline microstructure by suppressing recovery processes and reducing the grain boundary mobility. A very low intensity of aluminium deformation texture is observed in this as-extruded alloy. The volume of 12 %  $\text{Al}_4\text{C}_3$  with mean particles size 30nm and mean free path between particles 165 nm provides restrain of the dislocations motion in the Al matrix by the attractive interaction between dislocations and particles during extrusion.

2. The microstructure was unchanged in both materials after annealing at 773 K during 1 hour. By in situ measuring at 773 K the mean crystallite sizes increase, the values of the microstrain and of the dislocations density decrease in both materials in comparison to the initial state. After cooling to the ambient temperature all these parameters return in

practice to the values in initial state. The texture measured after extrusion is stable to 773 K in both materials. Both amounts of  $\text{Al}_4\text{C}_3$  dispersoid insure the thermal stability of microstructure of analyzed materials to 773 K.

#### ACKNOWLEDGEMENT

The authors would like to acknowledge the Slovak Grant Agency for Science (Grants No. 2/7196/29 and 2/0105/08) for the financial support.

#### REFERENCES

1. F. G. Lovshenko and G. Jangg, *Powder Metallurgy and Metal Ceramics*, **17**, (9), 686 (1978).
2. H. Hallem, B. Forbord and K. Marthinsen, *Mater. Sci. Eng. A* **387-389**, 940 (2004).
3. T. Weissgärber and B. F. Kieback, *Journal of Metastable and Nanocrystalline Materials*, **8**, 275 (2000).
4. G. Jangg, M. Šlesár, M. Besterci and J. Zbiral, *Werkstofftechnik*, **20**, 226 (1989).
5. H. P. Klug and L. E. Alexander, *X-ray Diffraction Procedures*. J. Wiley & Sons. New York (1974).
6. M. Diot, J. J. Funderberger, M. J. Philipe, J. Wégria and C. Esling, *Scripta Materialia*, **39**, (11), 1623 (1989).
7. C. S. Barret, T.B. Massalski, *Structure of Metals*, Pergamon, Oxford (1980).
8. T. Hasegawa, T. Miura, T. Takahashi and T. Yakou, *ISIJ International*, **32**, (8), 905 (1992).
9. J. Ďurišin, K. Ďurišinová, M. Orolinová and M. Besterci, *High Temperature Materials and Processes*, **25** (3), 149 (2005).
10. J. Gubicza and T. Ungár, *Z. Kristallogr.*, **222**, 567 (2007).
11. W. Woo, L. Balogh, T. Ungár, H. Choo and Z. Feng, *Materials Science and Engineering A*, **498**, 308 (2008).
12. Y. Estrin, M. Janecek, G.I. Raab, R.Z. Valiev and A. Zi, *Metallurgical and Materials Transactions A*, **38A**, 1906 (2007).
13. Y. S. Li, Y. Zhang, N. R. Tao and K. Lu, *Acta Materialia*, article in press.

